Sensors and Materials, Vol. 29, No. 4 (2017) 419–427
MYU Tokyo

S & M 1335

Application of Adaptive α-β-γ and α-β-γ-δ Filters to Tracking Systems

Tsan-Ying Yu and Chun-Mu Wu[1*]

Department of Electrical Engineering, Kao Yuan University,
No. 1821, Jhongshan Rd., Lujhu District, Kaohsiung City 821, Taiwan, R.O.C.
[1]Department of Mechanical Engineering and Automation Engineering, Kao Yuan University,
No. 1821, Jhongshan Rd., Lujhu District, Kaohsiung City 821, Taiwan, R.O.C.

(Received August 30, 2016; accepted January 27, 2017)

Keywords: α-β-γ filter, α-β-γ-δ filter, tracking system, white noise, jerk motion

Handling measurement system noise and maneuvering noise is a major challenge in tracking systems. White noise is added to displacement and acceleration signals to simulate measurement system noise and maneuvering noise in tracking systems. In this paper, adaptive parameters are applied to α-β-γ and α-β-γ-δ filters for tracking systems. The simulation model is the jerk motion of a target, and the results show that the adaptive parameters of the α-β-γ-δ and α-β-γ filters reduced measurement system noise and maneuvering noise. Together they can maintain the position tracking accuracy effectively.

1. Introduction

Multitudinous applications such as air traffic control, missile interception, and antisubmarine warfare require employing discrete-time data to predict the kinematics of a dynamic object. The measures of performance, such as stability, transient response, noise, and maneuvering error, as functions of the parameters α and β were proposed by Sklansky(1) and Simpson.(2) Owing to its simplicity and low cost, the α-β tracker has become popular. Neal and Benedict(3) analyzed the α-β-γ filter and obtained an optimization of the relationship among α, β, and γ. In addition, Kalata(4) and Tenne and Singh(5,6) summarized many analytical results of α-β-γ filter behavior from several studies. Tenne and Singh(5,6) reported the optimal design of the third-order α-β-γ filter. Later, Lee *et al.*(7) developed a real-coded genetic algorithm in the α-β-γ filter to search for the optimal parameter values. The proposed method effectively improved the maneuverability and performance of the α-β-γ filter while keeping the noise level within an acceptable range. Han *et al.*(8) used a formula to derive the correlation characteristic of the innovation sequence outputted by an α-β-γ filter. A correction α-β-γ filtering algorithm was proposed to apply to the simulation of multiple targets.(9) The implementation of an α-β-γ filter applied in the measurement of a carrier Doppler was discussed by Jia *et al.*(10)

Wu *et al.*(11–13) have proposed an optimal design of an α-β-γ-δ filter to improve significantly the position tracking accuracy compared with the α-β-γ filter. Recently, Wu *et al.*(14) have presented a search method for adaptive parameters for α-β-γ and α-β-γ-δ filters using the absolute minimum of the acceleration error and jerk error for every time step and path tracking using an accelerometer

*Corresponding author: e-mail: wtm@cc.kyu.edu.tw
http://dx.doi.org/10.18494/SAM.2017.1524

ISSN 0914-4935

with α-β-γ and α-β-γ-δ filters.[15] In this paper, the application of adaptive α-β-γ and α-β-γ-δ filters to measurement system noise and maneuver noise in a tracking system is presented.

2. Mathematical Model

Consider a one-dimensional, position-velocity-acceleration-jerk discrete time target motion:

$$\begin{bmatrix} x(k+1) \\ \dot{x}(k+1) \\ \ddot{x}(k+1) \\ \dddot{x}(k+1) \end{bmatrix} = \begin{bmatrix} 1 & T & \frac{1}{2}T^2 & \frac{1}{6}T^3 \\ 0 & 1 & T & \frac{1}{2}T^2 \\ 0 & 0 & 1 & T \\ 0 & 0 & 0 & 1 \end{bmatrix} \begin{bmatrix} x(k) \\ \dot{x}(k) \\ \ddot{x}(k) \\ \dddot{x}(k) \end{bmatrix} + \begin{bmatrix} \frac{1}{6}T^3 \\ \frac{1}{2}T^2 \\ 1 \\ 0 \end{bmatrix} w(k) \tag{1}$$

When the motion is not considered by a jerk model, the equation can be simplified as

$$\begin{bmatrix} x(k+1) \\ \dot{x}(k+1) \\ \ddot{x}(k+1) \end{bmatrix} = \begin{bmatrix} 1 & T & \frac{1}{2}T^2 \\ 0 & 1 & T \\ 0 & 0 & 1 \end{bmatrix} \begin{bmatrix} x(k) \\ \dot{x}(k) \\ \ddot{x}(k) \end{bmatrix} + \begin{bmatrix} \frac{1}{2}T^2 \\ T \\ 1 \end{bmatrix} w(k), \tag{2}$$

$$\text{Measurement: } z(k) = x(k) + n(k),$$

where $x(k)$ is the position at time k, $v(k) = \dot{x}(k)$ is the velocity at time k, $v(k) = \ddot{x}(k)$ is the acceleration at time k, $v(k) = \dddot{x}(k)$ is the jerk state at time k, T is the time step or time increment, $w(k)$ is an unknown target maneuver, and $n(k)$ is the measurement noise. The unknown target maneuvers $w(k)$ are modeled by a zero-mean, white stationary noise process. The measurement noise $n(k)$ is modeled by a zero-mean, white stationary noise process and is independent of the maneuvering noise.

The α-β-γ filter is a third-order tracker capable of predicting the object's next position and velocity by tracking the current and past positions and velocities.

The equations are

$$x_p(k+1) = x_s(k) + Tv_s(k) + \frac{1}{2}T^2 a_s(k) + \frac{1}{6}T^3 w(k), \tag{3}$$

$$v_p(k+1) = v_s(k) + Ta_s(k) + \frac{1}{2}T^2 w(k), \tag{4}$$

$$a_p(k+1) = a_s(k) + Tw(k), \tag{5}$$

where T is time step or time increment, x is position, v is velocity, and a is acceleration; the subscripts p and s denote the predicted and smoothed values, respectively.

The parameters are derived on the basis of previous prediction and the weighted innovation from the following:

$$x_s(k) = x_p(k) + \alpha[x_o(k) + n(k) - x_p(k)], \tag{6}$$

$$v_s(\mathrm{k}) = v_p(k) + \frac{\beta}{T}[x_o(k) + n(k) - x_p(k)], \tag{7}$$

$$a_s(k) = a_p(k-1) + \frac{\gamma}{2T^2}[x_o(k) + n(k) - x_p(k)], \tag{8}$$

where subscript o denotes the exact value. In mathematics and signal processing, the Z-transform converts a discrete time-domain signal, which is a sequence of real or complex numbers, into a complex frequency-domain representation. It is like a discrete equivalent of the Laplace transform. Just as analog filters are designed using the Laplace transform, the recursive digital filters are developed with a parallel technique called the Z-transform.

From Eqs. (3) to (8), the ratio $\frac{x_p}{x_o}$ is applied and solved using the Z-transform. The transfer function in the z-domain is given by

$$G(z) = \frac{x_p}{x_o} = \frac{\alpha + (-2\alpha - \beta + \frac{\gamma}{4})z + (\alpha + \beta + \frac{\gamma}{4})z^2}{z^3 + (\alpha + \beta + \frac{\gamma}{4} - 3)z^2 + (-2\alpha - \beta + \frac{\gamma}{4} + 3)z + \alpha - 1}. \tag{9}$$

Jury's Stability Test (1987) yields the constraints on α, β, and γ parameters for the α-β-γ filter as follows. This test is also used to find the stability domain for the characteristic polynomial (CP) of Eq. (9).

$$0 < \alpha < 2 \tag{10}$$

$$0 < \beta < \frac{13}{6}(4 - 2\alpha) \tag{11}$$

$$0 < \gamma < \frac{4\alpha\beta}{2 - \alpha} \tag{12}$$

To improve tracking accuracy, the mathematical equations of a fourth-order α-β-γ-δ filter target tracker included in predicting acceleration are given by

$$x_p(k+1) = x_s(k) + Tv_s(k) + \frac{1}{2}T^2 a_s(k) + \frac{1}{6}T^3 j_s(k) + \frac{1}{6}T^3 w(k), \tag{13}$$

$$v_p(k+1) = v_s(k) + Ta_s(k) + \frac{1}{2}T^2 j_s(k) + \frac{1}{2}T^2 w(k), \tag{14}$$

$$a_p(k+1) = a_s(k) + Tj_s(k) + Tw(k), \tag{15}$$

where

$$x_s(k) = x_p + \alpha[x_o(k) + n(k) - x_p(k)], \tag{16}$$

$$v_s = v_p(k) + \frac{\beta}{T}[x_o + n(k) - x_p(k)], \tag{17}$$

$$a_s(k) = a_p(k) + \frac{\gamma}{2T^2}[x_o + n(k) - x_p(k)], \tag{18}$$

$$j_s(k) = j_s(k-1) + \frac{\delta}{6T^3}[x_o(k) + n(k) - x_p(k)]. \tag{19}$$

Jury's Stability Test yields the constraints on α, β, γ, and δ parameters for the α-β-γ-δ filter as follows:

$$G(z) = \frac{x_p}{x_o} = \frac{(\alpha + \beta + \frac{\gamma}{4} + \frac{\delta}{36})z^3 + (-3\alpha - 2\beta + \frac{\delta}{9})z^2 + (3\alpha + \beta - \frac{\gamma}{4} + \frac{\delta}{36})z - \alpha}{z^4 + (\alpha + \beta + \frac{\gamma}{4} + \frac{\delta}{36} - 4)z^3 + (-3\alpha - 2\beta + \frac{\delta}{9} + 6)z^2 + (3\alpha + \beta - \frac{\gamma}{4} + \frac{\delta}{36} - 4)z + (1 - \alpha)} \tag{20}$$

$$0 < \alpha < 2 \tag{21}$$

$$0 < \beta < \frac{13}{6}(4 - 2\alpha) \tag{22}$$

$$0 < \gamma < \frac{4\alpha\beta}{2 - \alpha} \tag{23}$$

$$0 < \delta < 24(2 - \alpha) \tag{24}$$

3. Optimal Design of the *α-β-γ* and *α-β-γ-δ* filters

In this study, a method of searching for the adaptive parameter was applied to optimize the design of the α-β-γ and α-β-γ-δ filters. Four evenly spaced elements are created in the interval of ranges for each of the α, β, and γ parameters, and six evenly spaced elements are created in the interval of the range for the δ parameter because of its large range. The α-β-γ filter requires 64 runs to compute Eqs. (10)–(12). The optimal design minimizes the absolute value of the acceleration error $|\ddot{x}_s(k) - \ddot{x}_o(k)|$ to find the optimal parameter $(\alpha^*, \beta^*, \gamma^*)$ for every time step. The absolute value of the acceleration error is a function of α, β, and γ. First, we supply the same parameters β^* and γ^*. Then we use three-point $(\alpha^1, \alpha^*, \alpha^1)$ curve fitting to find the local optimal parameter $\hat{\alpha}$; α^1 and α^2 are the neighboring levels of the α^* parameter.

$$\begin{aligned} f(\alpha^1, \beta^*, \gamma^*) &= \lambda_1 \cdot \alpha^1 \cdot \alpha^1 + \lambda_2 \cdot \alpha^1 + \lambda_3 \\ f(\alpha^*, \beta^*, \gamma^*) &= \lambda_1 \cdot \alpha^* \cdot \alpha^* + \lambda_2 \cdot \alpha^* + \lambda_3 \\ f(\alpha^2, \beta^*, \gamma^*) &= \lambda_1 \cdot \alpha^2 \cdot \alpha^2 + \lambda_2 \cdot \alpha^2 + \lambda_3 \end{aligned} \tag{25}$$

When the following two conditions are satisfied, we can determine the local optimal parameter $\hat{\alpha} = -0.5 \cdot \dfrac{\lambda_2}{\lambda_1}$:

$$f(\alpha^*, \beta^*, \gamma^*) \le f(\alpha^1, \beta^*, \gamma^*) \text{ and } f(\alpha^*, \beta^*, \gamma^*) \le f(\alpha^2, \beta^*, \gamma^*). \tag{26}$$

Finally, we use the same method to find $\hat{\beta}$ and $\hat{\gamma}$.

The α-β-γ-δ filter requires 384 runs to compute Eqs. (21)–(24). The optimal design minimizes the absolute value of the jerk error $|\dddot{x}_s(k) - \dddot{x}_o(k)|$ to find the optimal parameters $(\alpha^*, \beta^*, \gamma^*, \delta^*)$ and the local optimal parameters $\hat{\alpha}$, $\hat{\beta}$, $\hat{\gamma}$, $\hat{\delta}$ for every time step.

4. Simulation Results

A simulation was performed for the α-β-γ and α-β-γ-δ filters. The low and high ends of each range are determined by checking the constraints listed in Eqs. (10)–(12) and (21)–(24), respectively. Assuming that the track of the target is jerk motion, the measured position x_x, y_x is applied with a white gauss noise with $SNR = 5$, the motion time is from 0 to 100 s, and the initial conditions are $j_x(0) = 0$ m/s³, $j_y(0) = 0$ m/s³, $a_x(0) = 0$ m/s², $a_y(0) = 0$ m/s², $v_x(0) = 200$ m/s, $v_y(0) = 200$ m/s, $x_x(0) = 1000$ m and $y_x(0) = -1000$ m. The target tracking motion equations are as follows.

1. During $10 \le t < 20$ s, $j_x(t) = -2$ m/s³, $j_y(t) = -1$ m/s³
2. During $20 \le t < 30$ s, $j_x(t) = 4$ m/s³, $j_y(t) = 2$ m/s³
3. During $30 \le t < 40$ s, $j_x(t) = -4$ m/s³, $j_y(t) = -2$ m/s³
4. During $40 \le t < 50$ s, $j_x(t) = 2$ m/s³, $j_y(t) = 2$ m/s³
5. During $50 \le t < 60$ s, $j_x(t) = -2$ m/s³, $j_y(t) = -2$ m/s³
6. During $60 \le t < 70$ s, $j_x(t) = 4$ m/s³, $j_y(t) = 2$ m/s³
7. During $70 \le t < 80$ s, $j_x(t) = -2$ m/s³, $j_y(t) = -2$ m/s³
8. During $80 \le t < 90$ s, $j_x(t) = 4$ m/s³, $j_y(t) = 2$ m/s³
9. During $90 \le t$, $j_x(t) = -4$ m/s³, $j_y(t) = -1$ m/s³

The simulation results of the tracker motion at $T = 0.2$ with both filters are shown in Figs. 1–9. Each error was calculated for five different time steps (i.e., $T = 0.2$, 0.1, 0.05, 0.025, and 0.0125).

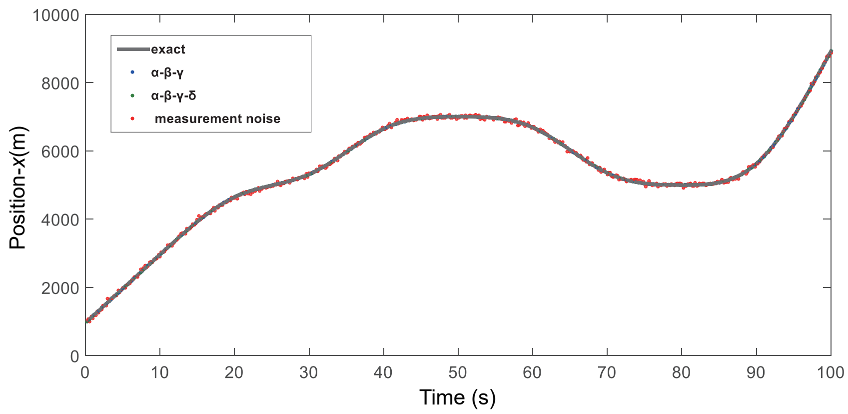

Fig. 1. (Color online) Position-x tracking plot at $T = 0.2$ for the α-β-γ and α-β-γ-δ filters.

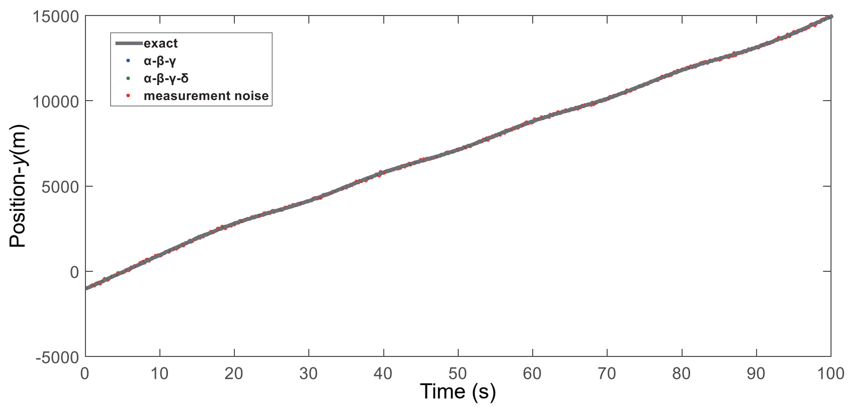

Fig. 2. (Color online) Position-y tracking plot at $T = 0.2$ for the α-β-γ and α-β-γ-δ filters.

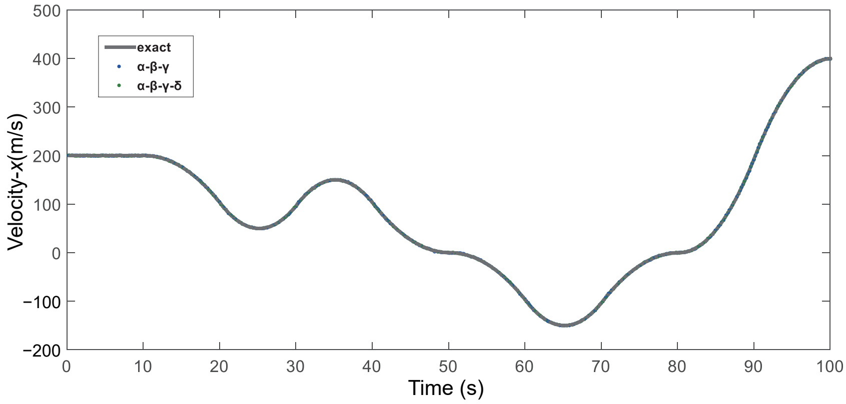

Fig. 3. (Color online) Velocity-x tracking plot at $T = 0.2$ with the α-β-γ and α-β-γ-δ filters.

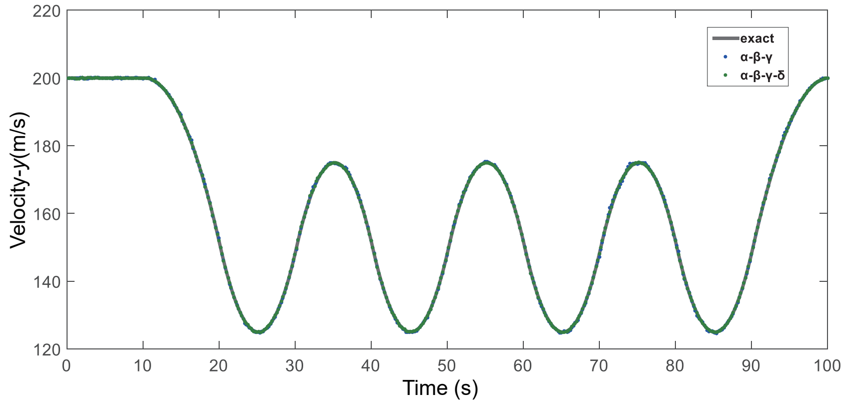

Fig. 4. (Color online) Velocity-y tracking plot at $T = 0.2$ with the α-β-γ and α-β-γ-δ filters.

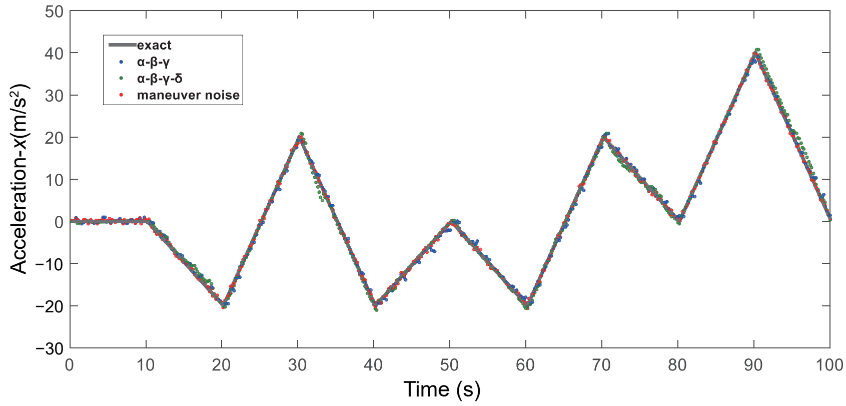

Fig. 5. (Color online) Acceleration-x tracking plot at $T = 0.2$ for the α-β-γ and α-β-γ-δ filters.

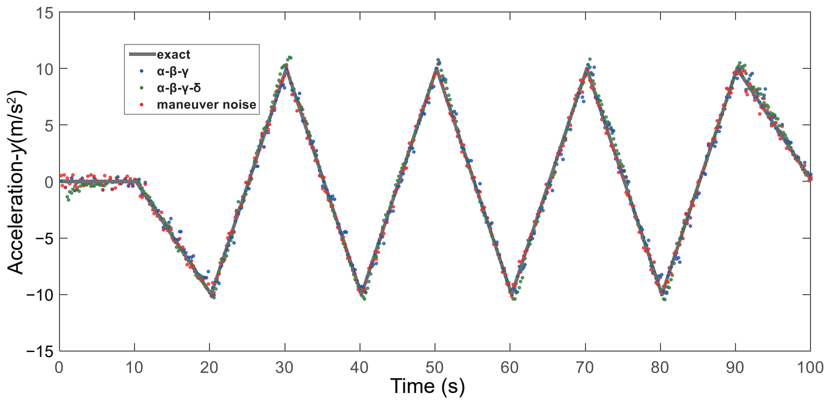

Fig. 6. (Color online) Acceleration-y tracking plot at $T = 0.2$ for the α-β-γ and α-β-γ-δ filters.

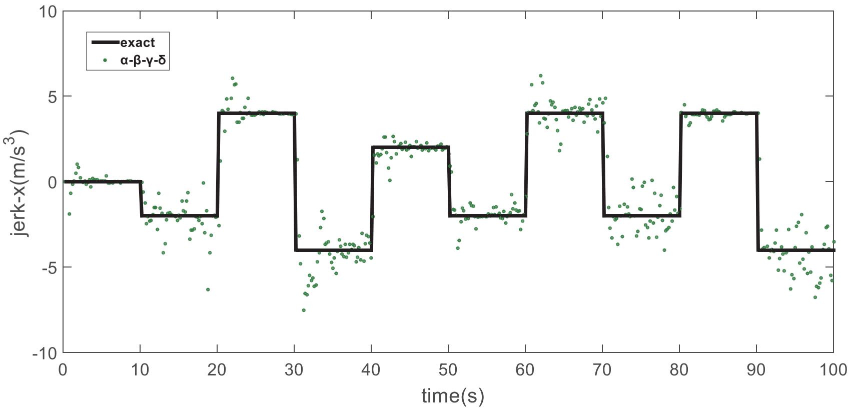

Fig. 7. (Color online) Jerk-x tracking plot at $T = 0.2$ for the α-β-γ-δ filter.

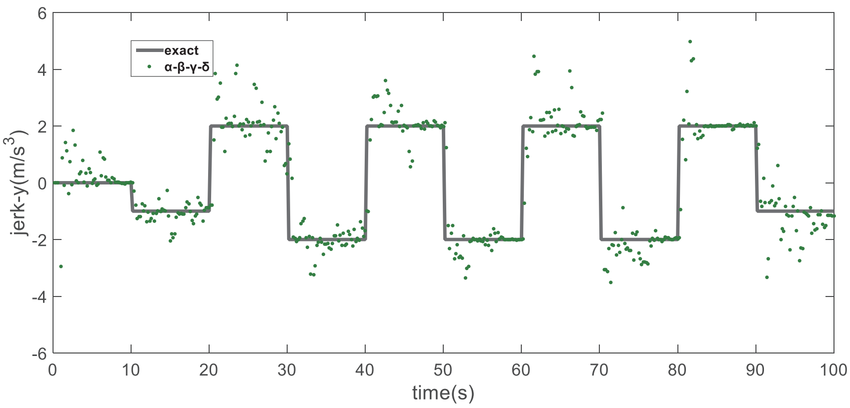

Fig. 8. (Color online) Jerk-y tracking plot at $T = 0.2$ for the α-β-γ-δ filter.

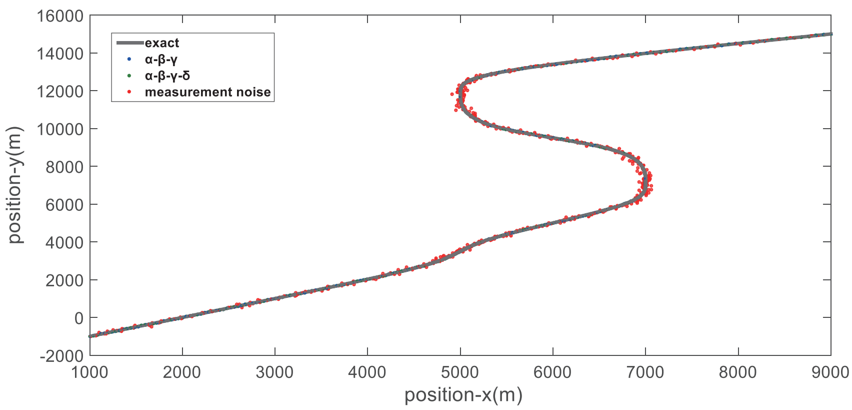

Fig. 9. (Color online) Path tracking plot at $T = 0.2$ for the α-β-γ and α-β-γ-δ filters.

Tables 1 and 2 summarize the tracking errors on the L_2 norm and L_{max} norm using the α-β-γ and α-β-γ-δ filters at each time step, respectively. The accuracy improvement is shown in each table. Tables 3 and 4 compare the tracking position errors on the L_2 norm and L_{max} norm between different time step for the α-β-γ and α-β-γ-δ filters.The smaller the time step, the smaller the error. Meanwhile, the smaller the time step, the more the improvement of L_2 and L_{max}. These simulations demonstrated that the α-β-γ-δ filter outperforms the α-β-γ filter at every time step. Clearly, a fourth-order target tracker of the α-β-γ-δ filter achieves a significantly better tracking accuracy than that of the α-β-γ filter.

Table 1
Comparisons of tracking position error on L_2 between *α-β-γ* and *α-β-γ-δ* filters.

Time step	*α-β-γ*	*α-β-γ-δ*	Improvement (%)
$T = 0.2$	4.2008e−003	2.1852e−003	92.2
$T = 0.1$	5.2863e−004	2.9665e−004	78.2
$T = 0.05$	8.7292e−005	2.0347e−005	329.0
$T = 0.025$	1.4708e−005	2.5308e−006	418.2
$T = 0.0125$	2.5829e−006	8.0670e−008	3101.8

Table 2
Comparisons of tracking position error on L_{max} between *α-β-γ* and *α-β-γ-δ* filters.

Time step	*α-β-γ*	*α-β-γ-δ*	Improvement (%)
$T = 0.2$	3.8833e−01	1.9120e−01	103.1
$T = 0.1$	9.9434e−02	7.2576e−02	37.0
$T = 0.05$	1.9723e−02	8.4185e−03	134.3
$T = 0.025$	6.2509e−03	1.7183e−03	263.8
$T = 0.0125$	1.4152e−03	1.1872e−04	1092.0

Table 3
Comparisons of tracking position error on L_2 between different time steps for *α-β-γ* and *α-β-γ-δ* filters.

Time step	*α-β-γ*	Improvement (%)	*α-β-γ-δ*	Improvement (%)
$T = 0.2$	4.2008e−003	—	2.1852e−003	—
$T = 0.1$	5.2863e−004	7.37	2.9665e−004	2.63
$T = 0.05$	8.7292e−005	14.58	2.0347e−005	8.62
$T = 0.025$	1.4708e−005	8.04	2.5308e−006	4.90
$T = 0.0125$	2.5829e−006	31.37	8.0670e−008	14.47

Table 4
Comparisons of tracking position error on L_{max} between different time steps for *α-β-γ* and *α-β-γ-δ* filters.

Time step	*α-β-γ*	Improvement (%)	*α-β-γ-δ*	Improvement (%)
$T = 0.2$	3.8833e−01	—	1.9120e−01	—
$T = 0.1$	9.9434e−02	7.95	7.2576e−02	3.91
$T = 0.05$	1.9723e−02	6.06	8.4185e−03	5.04
$T = 0.025$	6.2509e−03	5.94	1.7183e−03	3.16
$T = 0.0125$	1.4152e−03	5.69	1.1872e−04	4.42

5. Conclusions

An *α-β-γ-δ* filter was examined and compared with an *α-β-γ* filter by experimental tests in a path tracking system. The error and reliability of the path tracking systems were evaluated in three different experiments. All mean square errors and maximum errors were very small; in particular, the errors resulting from the *α-β-γ-δ* filter were much smaller than those from the *α-β-γ* filter in all experiments. There is much evidence to indicate that the *α-β-γ-δ* filter is more efficient than the *α-β-γ* filter. The *α-β-γ-δ* filter is a robust prediction technique and reduces the estimation error to a minimum. It could be applied indoors and in restricted environments. It also can be combined with path tracking for greater accuracy and more widespread applications.

References

1 J. Sklansky: IRE Rev. **2** (1957) 163.
2 H. Simpson: IEEE Trans. Autom. Control **8** (1963) 182.
3 S. Neal and T. Benedict: IEEE Trans. Autom. Control **12** (1967) 315.
4 P. R. Kalata: IEEE Trans. Aerosp. Electron. Syst. **20** (1984) 174.
5 D. Tenne and T. Singh: Proc. IEEE Int. Conf. Control Applic. (IEEE, 1999) Vol. 2, p. 1342.
6 D. Tenne and T. Singh: Proc. Amer. Control Conf. **6** (2000) 4348.
7 T. E. Lee, J. P. Su, and K. W. Yu: The Second Int. Conf. Innov. Comput. Inf. Control (2007) p. 336.
8 W. Han, X. Z. Huang, and Z. Y. Xiaobin: Comput. Eng. Appl. J. **49** (2013) 156.
9 R. F. Zhu and J. Zhang: J. Tianjin Univ. Tech. Edu. **3** (2013) 004.
10 W. Jia, L. Wang, and H. Shi: Aerosp. Control **31** (2013) 6.
11 C. M. Wu, C. K. Chang, and T. T. Chu: J. Chin. Soc. Mech. Eng. **30** (2009) 467.
12 C. M. Wu, C. K. Chang, and T. T. Chu: Math. Comput. Simul. **81** (2011) 1785.
13 C. M. Wu, P. P. Lin, Z. Y. Han, and S. R. Li: Int. J. Autom. Comput. **7** (2010) 247.
14 C. M. Wu: Adv. Mech. Eng. **8** (2016) 1.
15 C. M. Wu and T. Y. Yu: Sens. Mater. **28** (2016) 433.

About the Authors

Tsan-Ying Yu received his B.S. degree from Tatung Institute of Technology, Taiwan, in 1986, his M.S. degree from the National Chung Cheng University, Taiwan, in 1992 and his Ph.D. degree from the National Kaohsiung First University of Science and Technology, Taiwan, in 2012. From 1993 to 2011, he was a lecturer at Koa Yuan University, Taiwan. Since 2012, he has been an associate professor at Koa Yuan University. His research interests are in pattern recognition and image processing.

Chun-Mu Wu received his B.S. and M.S. degrees from Tamkang University, Taiwan, in 1981 and 1983, and his Ph.D. degree from National Cheng Kung University, Taiwan in 1993. From 1993 to 2016, he was an associate professor at Koa Yuan University, Taiwan. Since 2016, he has been an professor at Koa Yuan University. His research interests are in numerical analysis, heat transfer analysis, optimal control, and robotics.